Journal of the Korean Crystal Growth and Crystal Technology
Vol. 15, No. 5 (2005) 188-192

Crystal growth and pinning enhancement of directionally melt-textured $(Y_{0.5}Nd_{0.25}Sm_{0.25})Ba_2Cu_3O_y$ oxides in air

So-Jung Kim†

Department of Electrical and Electronic Engineering, Hanzhong University, Donghae 240-713, Korea

(Received September 27, 2005)
(Accepted October 7, 2005)

Abatract High T_c $(Y_{0.5}Nd_{0.25}Sm_{0.25})Ba_2Cu_3O_y$ [(YNS)-123] superconductors with/without CeO_2 additive were systematically investigated by the zone melt growth process in air. Cylindrical green rods of (YNS)-123 oxides were fabricated by cold isostatic pressing (CIP) method using rubber mould. A sample prepared by this method showed well-textured microstructure, and $(Y_{0.5}Nd_{0.25}Sm_{0.25})_2BaCuO_5$ [(YNS)211] nonsuperconducting inclusions were uniformly dispersed in large $(Y_{0.5}Nd_{0.25}Sm_{0.25})Ba_2Cu_3O_y$ [(YNS)123] superconducting matrix. In this study, optimum melting temperature and growth rate were 1100°C and 3 mm/hr, respectively. The directionally melt-textured (YNS)-123 sample with CeO_2 additive showed an onset critical temperature (T_c) $T_c \geq 93$ K and sharp superconducting transition.

Key words $(Y_{0.5}Nd_{0.25}Sm_{0.25})Ba_2Cu_3O_y$, Zone melt growth, $(Y_{0.5}Nd_{0.25}Sm_{0.25})_2BaCuO_5$, CIP, CeO_2 additive.

1. Introduction

Large single-grain $REBa_2Cu_3O_y$ 'RE-123' (REBCO, RE: Nd, Sm, Eu, Gd) superconductors are promising materials for cryogenic applications since they demonstrate superior superconducting parameters such as critical current density (J_c) and critical temperature (T_c), compared to Y-Ba-Cu-O (YBCO) bulks. Additionally, the melt-textured high T_c superconductor enables flux pinning to improve by introducing fine dispersion of second phase precipitate, such as Y_2BaCuO_5 (Y211) and RE_2BaCuO_5 (RE211), which acts as strong pinning center. Recent advances in melt-growth techniques enabled the fabrication of large single grain REBCO bulk superconductors with high current-carrying capability through the enhancement of flux pinning and the reduction of weak links. Zone melt growth process is a good fabrication method to eliminate the weak links and obtain large grain with good alignment so as to increase critical current density [1-5]. In the zone melt growth process, as there is no contact between the liquid and the support, these liquid losses are avoided. So, this process is an efficient way for processing in YBCO and REBCO bars with a high and sharp superconducting transition. In the melt-textured YBCO and REBCO systems, among various means to reduce the average 211 particle size, there are certain additions which minimize coarsening of the 211 and help to refine 211 size, with Ce and Pt-based additives being effective in this regard. In particular, CeO_2 has demonstrated a remarkable RE211 refining effect. Recently, several research groups have reported that RE-123 systems where two or three rare-earth elements $(Nd_{0.33}Eu_{0.33}Gd_{0.33})Ba_2Cu_3O_y$ (NEG123) are mixed can show very large values of critical current densities (J_c), when they are processed by oxygen controlled melt growth (OCMG) technique [6, 7]. However, the OCMG process has some drawbacks, including additional cost and equipment for commercialization. Unfortunately, in the solid solution $RE_{1+x}Ba_{2-x}Cu_3O_7$ system, RE elements, particularly Nd, can easily substitute into the Ba sites, leading to depressed T_c's when the solidification is performed in air. In this study, we reported grain growth and superconducting properties of (YNS)-123 composite oxides with/without CeO_2 additive prepared by zone melt growth process in air atmosphere and systematically investigated the microstructure of finely dispersed (YNS)211 nonsuperconducting inclusions in the (YNS)123 superconducting matrix.

2. Experimental Procedure

Zone melt growth process for fabricating (YNS)-123 composite oxides containing (YNS)211 second phase is as follows. High purity commercial powders of Y_2O_3, Nd_2O_3, Sm_2O_3, $BaCO_3$, and CuO powders were weighed in appropriate amounts and mixed in an agate mortar according to the nominal composition of $(Y_{0.5}Nd_{0.25}Sm_{0.25})Ba_2Cu_3O_y$

†Corresponding author
Tel: +82-33-520-9322
Fax: +82-33-521-9407
E-mail: sjkim@donghae.ac.kr

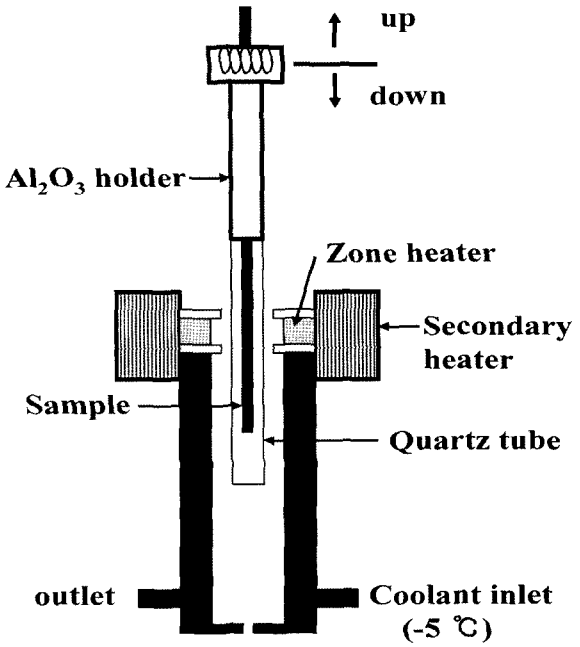

Fig. 1. Schematic illustrations of the experimental apparatus for zone melt growth method.

[(YNS)-123]. Precursor powders were thoroughly ground and calcined at 900°C for 30 h twice in air with intermediate grinding. It was reported that CeO_2 is effective for increasing the viscosity of the Ba-Cu-O melts and can act as a growth inhibitor for RE211 particles [8, 9]. For these reasons, 1 wt% CeO_2 was added. All these powders [(YNS)-123+(YNS)211+CeO_2] were mixed and milled with attrition for 6 h in acetone using zirconia balls with a rotation speed 450 rpm. The (YNS)-123 powders milled with attrition were dried in air, and then isostatically pressed at 200 MPa into a small cylindrical type (3 mm in inner diameter, 6 mm in outer diameter and 100 mm in length) using rubber mould. The preheated (930°C, 5 h) (YNS)-123 rod samples were processed in a vertical zone melting furnace, applying a thermal gradient (G) close to 200°C/cm. An unidirectional solidification was obtained by moving the sample upward through a hot zone (1100°C) at a rate of about 3 mm/h in air. The zone melt growth apparatus used in this study was shown in Fig. 1. The post-heat treatment was performed at 450°C oxygen gas atmosphere for 150 h in a separate tube furnace. Directionally melt grown sample of (YNS)-123 was cleaved into smaller sections (2~3 mm long) for characterization. The microstructure observations were performed on well polished surfaces of the samples by means of scanning electron microscopy (SEM), transmission electron microscopy (TEM), and high-resolution transmission electron microscopy (HR-TEM). Chemical composition of the matrix and secondary phase was determined by energy dispersive x-ray spectrometer (EDS) analysis. Superconducting properties were measured for H//c-axis in a Quantum Design MPMS SQUID magnetometer at various temperature from 10 K from 110 K.

3. Results and Discussion

Microstructure control of high temperature superconductors is the key parameter for successful industrial applications of these materials. In the REBCO bulk system, a large number of crystal defects are present in the RE123 matrix that can act as effective pinning centers [10]. Figure 2 shows photograph of the directionally melt grown (YNS)-123 crystal by zone melt growth process in air. Figure 3 shows SEM micrographs of the fracture cross section transverse to the long axis of the directionally melt-textured (YNS)-123 crystal viewed in Fig. 2. In Fig. 3, we can see that the thin (YNS)-123 platelets (plate-type grains) are oriented parallel to the long axis and that the platelets extend across the entire cross section of the directionally melt-textured rod crystal.

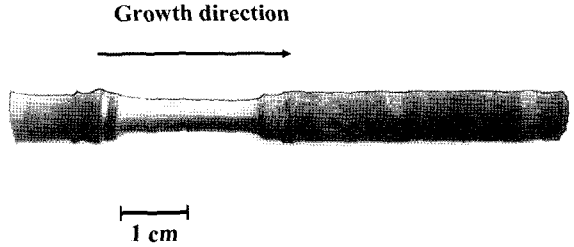

Fig. 2. Photograph of the directionally melt grown (YNS)-123 crystal.

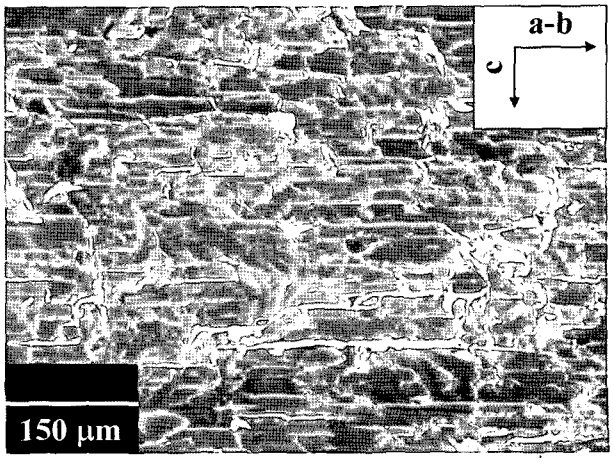

Fig. 3. SEM micrograph of the fracture cross section of the directionally melt-textured (YNS)-123 crystal viewed in Fig. 2.

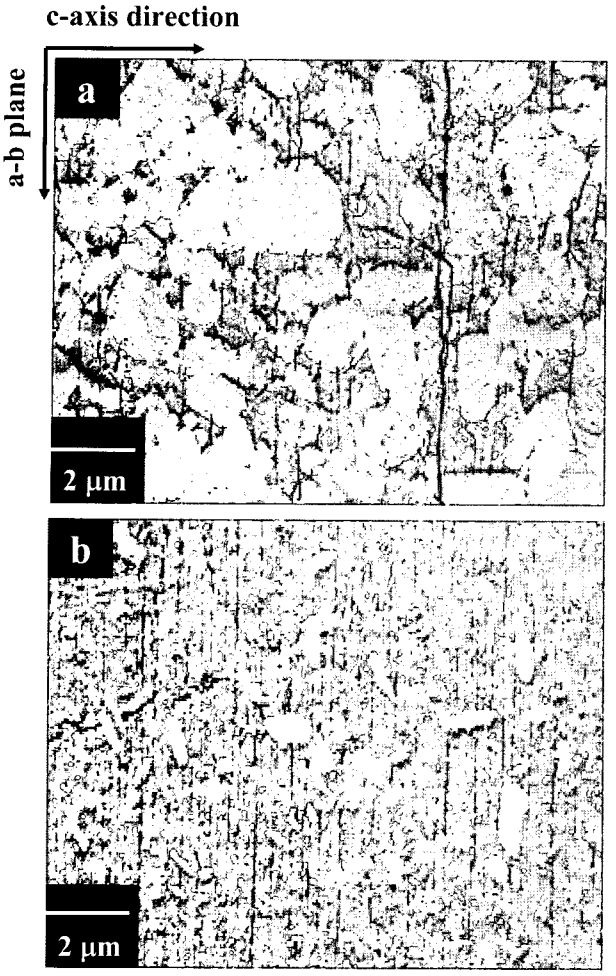

Fig. 4. SEM micrographs of the directionally melt-textured (a) (YNS)-123 and (b) (YNS)-123 crystal with 1 wt% CeO_2 additions. Note finely dispersed (YSN)211 inclusions are trapped into the (YNS)123 matrix with platelet crystals.

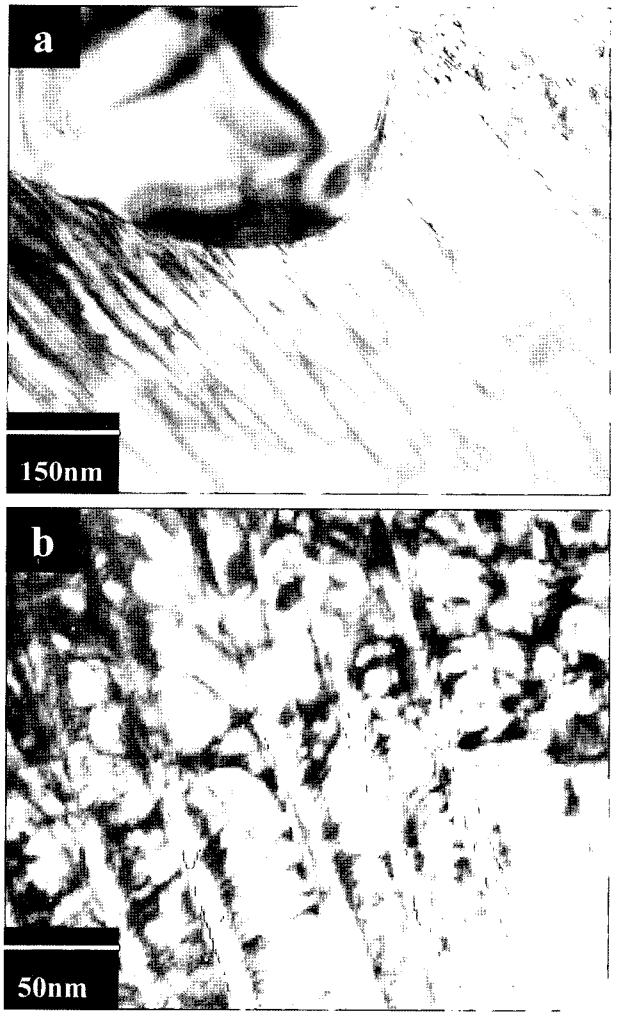

Fig. 5. TEM micrograph of the directionally melt-textured (YNS)-123 crystal with 1 wt% CeO_2 additive. The (YNS)211 inclusion, dense twin patterns, dislocations and nano-sized defects are seen in the image.

Figure 4 shows that uniform (YNS)211 inclusions are trapped within the (YNS)123 matrix, which have platelet structure. As can be seen in Fig. 4, in CeO_2 additive sample, the (YNS)211 inclusion size was remarkably reduced and the inclusions finely dispersed within the (YNS)123 matrix. In the melt-processed REBCO bulk system, the RE211 inclusions tend to coarsen in liquid (Ba-Cu-O) through the Ostwald ripening process. CeO_2 additive is effective in suppressing the growth of RE211 inclusions. It is evident that the size of the (YNS)211 inclusions is depressed by CeO_2 additive. This refinement of (YNS)211 inclusions is observed for all samples.

In the melt growth processed REBCO bulk system, the pinning provided by the nonsuperconducting particles of the RE211 phase is mainly effective at low magnetic fields and high temperature above 77 K. In this case, the interfaces between RE123 matrix and RE211 inclusions play an important role in the flux pinning, because the size of RE211 is much larger than the coherence length [10]. In order to obtain more detailed information on the (YNS)211 inclusion size and distribution, we performed transmission electron microscopy (TEM) on the same sample. TEM was performed on the sample annealed at 450°C for 100 h. Figure 5 shows TEM bright field image around the (YNS)211 inclusion of the (YNS)123 matrix viewed from a [001] direction. As can be seen in the Fig. 5b, the existence of nano defects and a high density of dislocations in addition to the twin structure are observed. Also, twin and twin boundaries having about 50 nm space can be observed in Fig. 5b.

Figure 6 shows HR-TEM image and selected area electron diffraction (SAED) patterns around the (YNS)123 matrix and the (YNS)211 inclusion viewed from a [001]

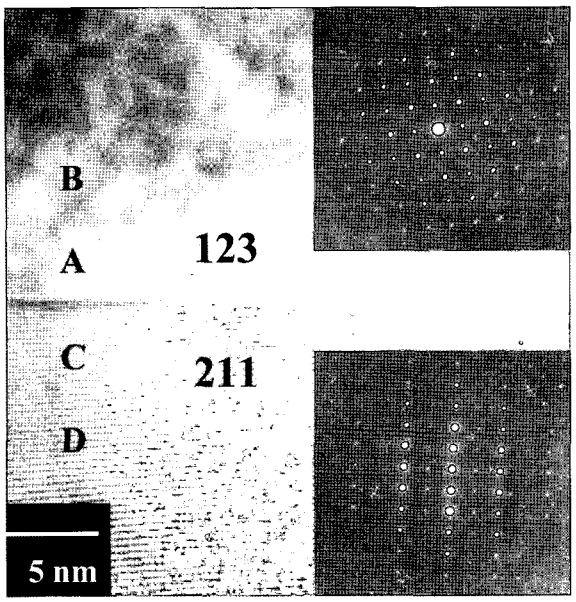

Fig. 6. High resolution TEM image and SAED patterns of the interface between a (YNS)211 inclusion and (YNS)123 matrix showing its shape and structure. The SAED patterns shown in the inset indicates trapped phases are nearly well crystallized, respectively.

direction. In Fig. 6, high resolution TEM image really showed clean interfaces between the (YNS)123 and (YNS)211 without any impurity phase. As shown in Fig. 6, (YNS)123 matrix and (YNS)211 inclusion are well crystallized, respectively. TEM-EDS analysis was performed on both the (YNS)123 matrix and (YNS)211 inclusions with different positions, shown in Fig. 6. As shown in Table 1, only homogeneous (YNS)123 and (YNS)211 are observed, and impurity phase of RE is not found. To increase pinning effect, total area of the interface should be important; smaller Y211 and RE211 inclusions are more efficient in enhancing flux pinning [10-13]. Figure 6 exhibits that the interface between (YNS)211 inclusion and (YNS)123 matrix is sharp. The sharp interface between the (YNS)123 and (YNS)211 as well as the substitution of RE for the half of Y in (YNS)-123 compound may provide more effective pinning centers than in Y-123 samples.

Table 1
TEM-EDS analysis on (YNS)123 matrix and (YNS)211 inclusion of as grown (YNS)-123 crystal shown in Fig. 6

Element (at. %)	(YNS)123 matrix		(YNS)211 inclusion	
	A	B	C	D
Y	2.893	2.951	11.676	10.543
Nd	3.037	3.181	5.899	6.149
Sm	2.873	2.919	4.889	4.797
Ba	17.571	17.745	11.721	11.668
Cu	23.665	23.951	10.663	10.652

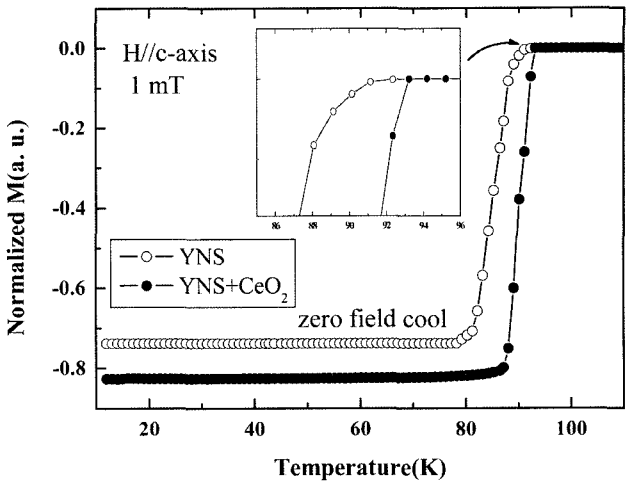

Fig. 7. Temperature dependence of the normalized magnetic susceptibility for the directionally melt-textured (YNS)-123 sample. The measurements were performed with zero-field cooled (ZFC) warming procedure with an applied field of 1 mT and for H//c-axis direction.

In order to find out how the sample consists of superconducting phase, magnetic susceptibility of the directionally melt-textured (YNS)-123 sample was measured. The field of 1 mT was applied parallel to the c-axis from 10 to 110 K in zero field cooled (ZFC). As shown in Fig. 7, the (YNS)-123 sample with CeO_2 additive shows a sharp superconducting transition at 93 K, indicating that the sample consists of a homogeneous superconducting phase. This result in attributed to, in part, the finely dispersive (YNS)211 inclusions which apparently act as effective pinning centers. It seems that the flux pinning mechanism by the fine (YNS)211 inclusion within the (YNS)123 matrix is more effective in improving superconducting properties of the (YNS)-123 phase than the coarse (YNS)211 inclusion.

4. Conclusions

In this paper, we have succeeded in the synthesis of directionally melt-textured (YNS)-123 superconductor with CeO_2 additive by the zone melt growth process in air atmosphere. The (YNS)211 nonsuperconducting inclusions, having spherical shape, are uniformly dispersed within (YNS)123 superconducting matrix. The directionally melt-textured (YNS)-123 crystal with 1 wt% CeO_2 additive as a sharp transition temperature of 93 K consists of homogeneous superconducting phase. The enhancement of flux pinning may be associated with the well-defined interface between (YNS)211 inclusions and (YNS)123

matrix as well as the substitution of RE for the half of Y site in (YNS)-123 compound. This result would be useful for the application fields of the high T_c bulk superconductors that require large critical current even at high magnetic field.

References

[1] P. McGinn, W. Chen, N. Zhu, M. Lanagan and U. Balanchandran, "Microstructure and critical current density of zone melt textured $YBa_2Cu_3O_{6+x}$", Appl. Phys. Lett. 57(14) (1990) 1455.

[2] F. Giovannelli, S. Marinel and I. Monot-Laffez, "Melt processing of (light rare earth)$Ba_2Cu_3O_y$ materials by the floating zone method", Supercond. Sci. Technol. 15 (2002) 533.

[3] A. Ubaldini, F. Giovannelli and I. Monot-Laffez, "$(RE_{0.33}Eu_{0.33}Gd_{0.33})Ba_2Cu_3O_y$ bars processed in air", Pysica C 33 (2002) 107.

[4] F. Giovannelli, S. Marinel and I. Monot-Laffez, "Properties of the $(Sm_{0.33}Eu_{0.33}Gd_{0.33})Ba_2Cu_3O_y$ superconductor prepared by different process in air", Supercond. Sci. Technol. 16 (2003) 444.

[5] S.J. Kim, "Flux pinning enhancement and irreversibility line of Sm doped YBCO superconductor by zone melt growth process", J. KIEEME (Korea) 5 (2004) 81 (in English).

[6] S. Awaji, N. Isono, K. Watanabe, M. Muralidhar, M. Murakami, N. Koshizuka and K. Noto, "High magnetic field transport properties of (Nd, Eu, Gd)$Ba_2Cu_3O_x$ bulk", Supercond. Sci. Technol. 17 (2004) S6.

[7] M. Muralidhar, N. Sakai, M. Jirsa and M. Murakami, "Fabrication and characterization of $LRE_{1+x}Ba_{2-x}Cu_3O_y$ (LRE: Nd, Eu, Gd, NEG) superconductors: a low oxygen partial pressure", Physica C 378 (2002) 646.

[8] C.J. Kim, H.W. Park, K.B. Kim and G.W. Hong, "New method of producing fine Y_2BaCuO_5 in the melt-textured Y-Ba-Cu-O system: attrition milling of $YBa_2Cu_3O_y$-Y_2BaCuO_5 powder and CeO_2 addition prior to melting", Supercond. Sci. Technol. 8 (1995) 652.

[9] M.P. Delamare, M. Hervieu, J. Wang, J. Provot, I. Monot, K. Verbist and G. Van Tendeloo, "Combination of CeO_2 and PtO_2 doping for strong enhancement of J_c under magnetic field in melt-textured superconductor YBaCuO", Physica C 262 (1996) 220.

[10] R. Cloots, T. Koutzarova, J.P. Mathieu and M. Ausloos, "From RE-211 to RE-123. How to control the final microstructure of superconducting single-domains", Supercond. Sci. Technol. 18 (2005). R59.

[11] S. Nariki, N. Sakai, M. Murakami and I. Hirabayashi, "High critical current density in Y-Ba-Cu-O bulk superconductors with very fine Y211 particles", Supercond. Sci. Technol. 17 (2004) S30.

[12] M.R. Koblischka, M. Muralidhar and M. Murakami, "Flux pinning sites in melt-processed $(Nd_{0.33}Eu_{0.33}Gd_{0.33})Ba_2Cu_3O_y$ superconductors", Physica C 337 (2000) 31.

[13] P.C. Heieh, S.Y. Chen, I.G. Chen and M.K. Wu, "Flux pinning at high magnetic field in melt-processed $SmBa_2Cu_3O_7$ with nanocrystalline Sm211/Nd422 additives", Supercond. Sci. Technol. 18 (2005) S111.